Supplementary Information

Self-improvement of solar water oxidation for the continuously-irradiated hematite photoanode

Zhongyuan Zhou,[a,b] Shaolong Wu,[*a,b] Chenhong Xiao,[a,b] Liujing Li,[a,b] Weijia Shao,[a,b] Hao Ding,[a,b] Long Wen,[c] and Xiaofeng Li[a,b]

[a]*School of Optoelectronic Science and Engineering & Collaborative Innovation Center of Suzhou Nano Science and Technology, Soochow University, Suzhou 215006, China*
[b]*Key Lab of Advanced Optical Manufacturing Technologies of Jiangsu Province & Key Lab of Modern Optical Technologies of Education Ministry of China, Soochow University, Suzhou 215006, China*
[c]*Institute of Nanophotonics, Jinan University, Guangzhou 511443, China*

[*]E-mail: shaolong_wu@suda.edu.cn

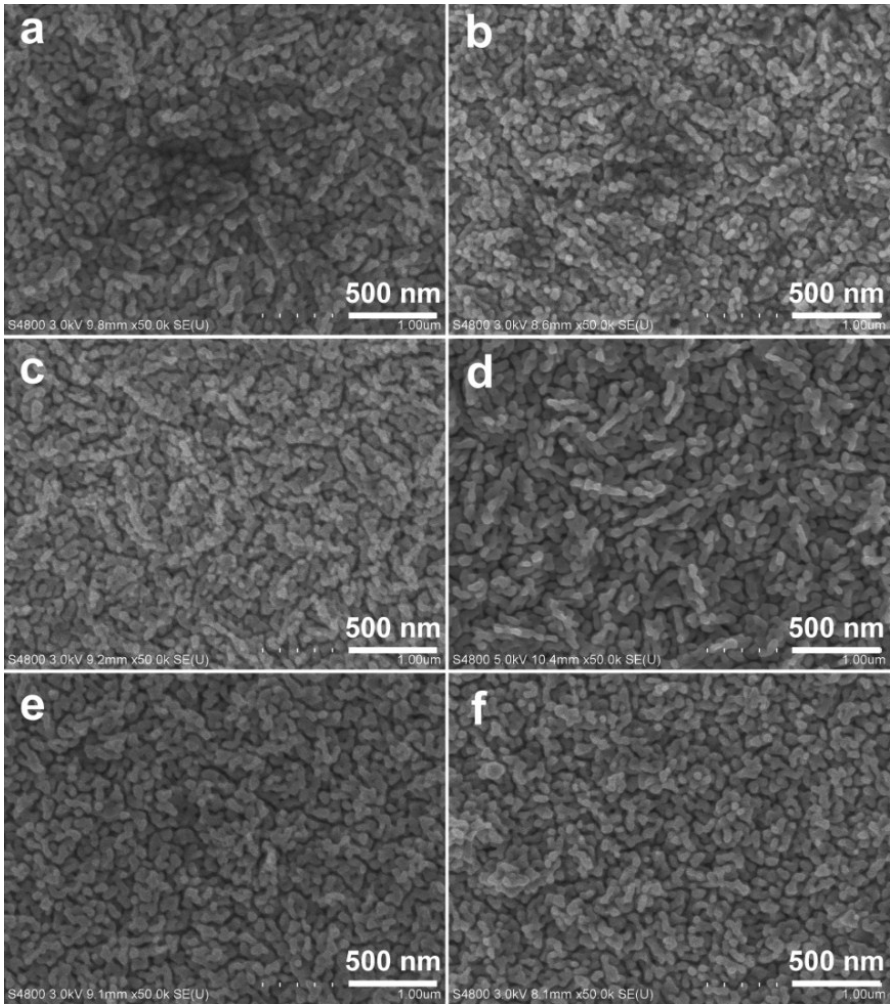

Fig. S1 SEM images of FTO/α-Fe_2O_3 (a and b), FTO/Sn@α-Fe_2O_3 (c and d) and FTO/TiO_2/Sn@α-Fe_2O_3 (e and f) photoanodes before and after PC for 12 h.

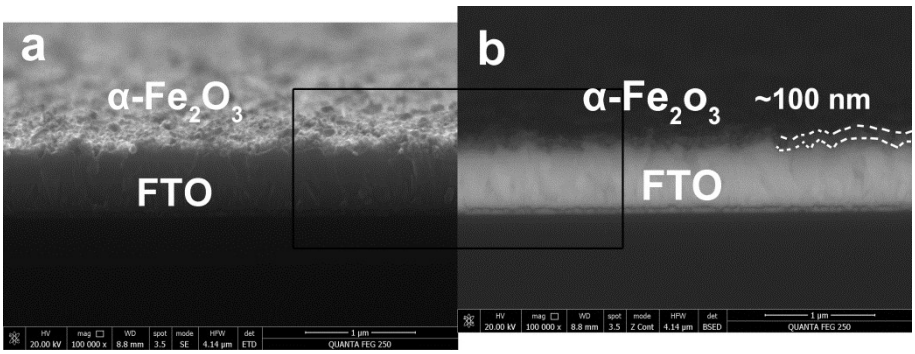

Fig. S2 Using SEM images of FTO/TiO_2/Sn@α-Fe_2O_3 photoanode to determine the α-Fe_2O_3 thickness.

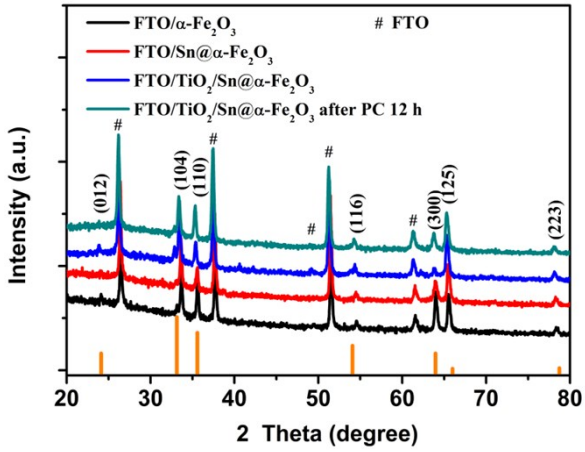

Fig. S3 XRD patterns of FTO/α-Fe_2O_3, FTO/Sn@α-Fe_2O_3 and FTO/TiO_2/Sn@α-Fe_2O_3 photoanodes before PC and FTO/TiO_2/Sn@α-Fe_2O_3 photoanode after PC for 12 h.

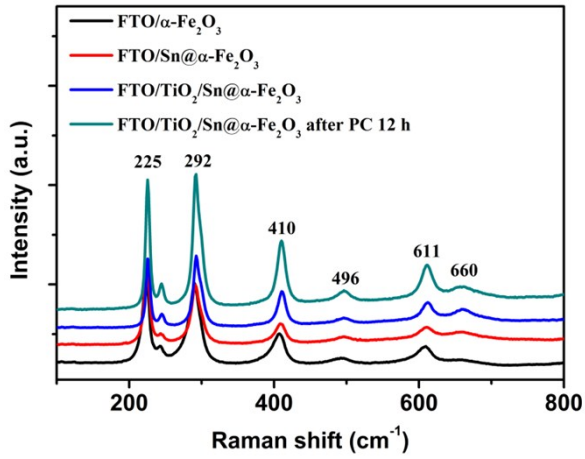

Fig. S4 Raman plots of FTO/α-Fe_2O_3, FTO/Sn@α-Fe_2O_3 and FTO/TiO_2/Sn@α-Fe_2O_3 photoanodes before PC and FTO/TiO_2/Sn@α-Fe_2O_3 photoanode after PC for 12 h.

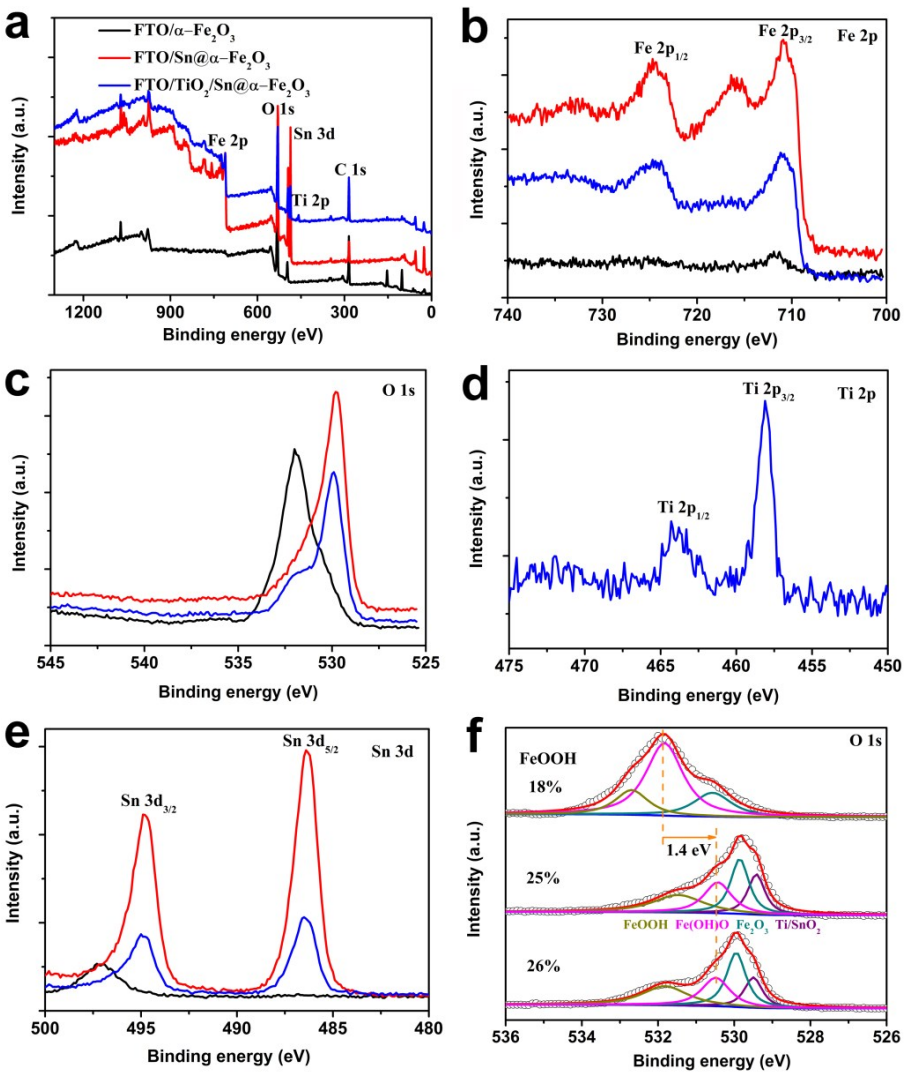

Fig. S5 XPS spectra of FTO/α-Fe_2O_3, FTO/Sn@α-Fe_2O_3 and FTO/TiO_2/Sn@α-Fe_2O_3 photoanodes before PC. In (b), the peaks of Fe $2p_{1/2}$ and Fe $2p_{3/2}$ indicate the typical values of Fe^{3+} in hematite. In (c), the different peaks of O 1s are caused by Sn and Ti doping from Sn dopant and an underlayer TiO_2. In (d), the peaks of Ti $2p_{1/2}$ and Ti $2p_{3/2}$ indicate that the Ti element exists in the FTO/TiO_2/Sn@α-Fe_2O_3 photoanode. In (e), the peaks of Sn $3d_{5/2}$ and Sn $3d_{3/2}$ suggest that the Sn element exists in the FTO/Sn@α-Fe_2O_3 and FTO/TiO_2/Sn@α-Fe_2O_3 photoanode. (f) The fitting profile O1s XPS spectra.

Table S1 A comparison of the PEC performances between our present photoanodes and the typical related photoanodes with PC effect.

Samples	$J_{ph@1.23\ V}$ (mA cm^{-2})			$J_{ph@1.5\ V}$ (mA cm^{-2})			U_{on} (V vs. RHE)			PC Conditions	Ref.
	Before PC	After PC	Improvement	Before PC	After PC	Improvement	Before PC	After PC	Improvement		
FTO/α-Fe_2O_3	0.051	0.123	0.072 (141%)	0.075	0.144	0.069 (92%)	-	-	-	AM 1.5G for 12 h in 1 M NaOH solution	This work
FTO/Sn@ α-Fe_2O_3	0.272	0.394	0.122 (45%)	0.419	0.777	0.358 (85%)	1.01	0.93	0.08	AM 1.5G for 12 h in 1 M NaOH solution	This work
FTO/TiO_2/ Sn@α-Fe_2O_3	0.69	1.12	0.43 (62%)	1.24	2.08	0.84 (68%)	0.95	0.85	0.1	AM 1.5G for 12 h in 1 M NaOH solution	**This work**
FTO/Ti@ α-Fe_2O_3	0.27	0.32	0.05 (17%)	0.35	0.4	0.05 (14%)	0.96	0.86	0.1	AM 1.5G for 70 h in 1 M NaOH solution	[1]
FTO/Fe_2TiO_5 /α-Fe_2O_3	1.62	2.02	0.4 (24%)	2.2	2.7	0.5 (22%)	0.9	0.9	0	AM 1.5G for 2.5 h in 1 M NaOH solution	[2]
FTO/SnO_2/ $BiVO_4$	1.3	3.3	2.0 (153%)	2.4	4.1	1.7 (70%)	0.7	0.4	0.3	AM 1.5G for 20 h in pH = 7 solution	[3,4]
FTO/SnO_2/ $BiVO_4$	1.0	1.0	0 (0%)	2.3	2.3	0 (0%)	0.75	0.75	0	AM 1.5G for 20 h in pH = 4 solution	[4]
FTO/SnO_2/ $BiVO_4$	1.1	4.3	3 (290%)	2.4	4.5	2.1 (87%)	0.75	0.25	0.5	AM 1.5G for 20 h in pH = 10 solution	[4]
FTO/$BiVO_4$	0.3	0.55	0.25 (83%)	-	-	-	1.0	0.8	0.2	AM 1.5G for 3 h in pH = 7 solution	[5]
FTO/$BiVO_4$	0.7	1.2	0.5 (71%)	0.95	1.5	0.55 (57%)	0.65	0.42	0.23	UV light for 20 h in air	[6]
FTO/WO_3	0.53	0.69	0.16 (30%)	0.6	0.76	0.16 (26%)	0.65	0.65	0	UV light for 4 h in air	[7]
TiO_2 nanotube	0.4	0.6	0.2 (50%)	0.4	0.6	0.2 (50%)	0.22	0.22	0	UV light for 1 h in air	[8]

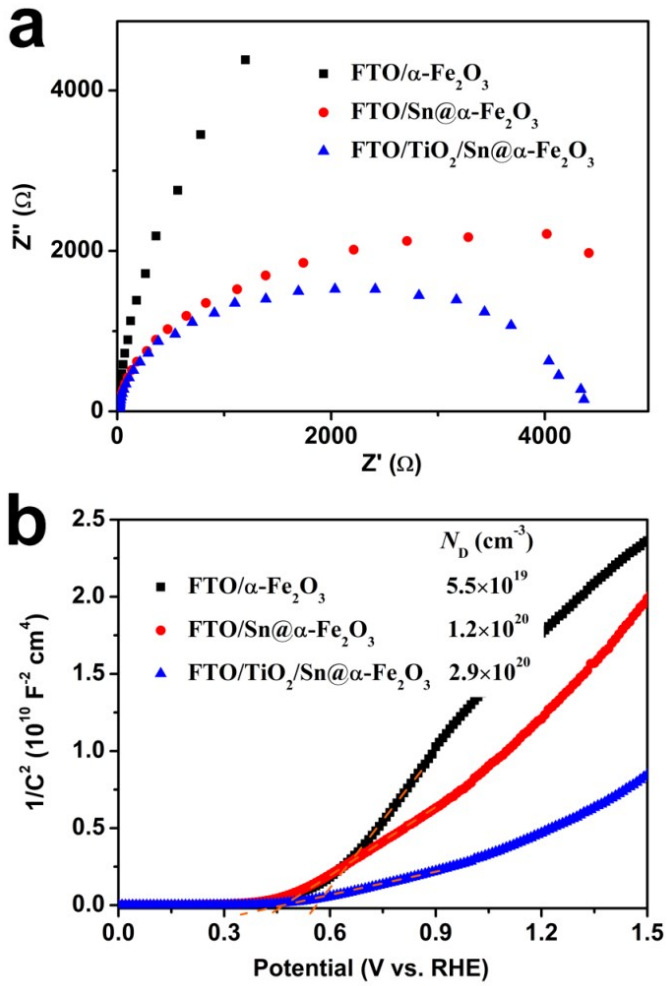

Fig. S6 PEIS and Mott-Schottky plots of FTO/α-Fe_2O_3, FTO/Sn@α-Fe_2O_3 and FTO/TiO_2/Sn@α-Fe_2O_3 photoanodes. Fig. S5a shows that the radius of the sample with Sn doping and a TiO_2 underlayer is getting smaller, implying that the resistance associated with charge trapping on the surface states and transferring into electrolyte is getting smaller.[9] So the introduced Sn doping and a TiO_2 underlayer in photoanode can reduce the trapping and transfer resistance.[10] The Mott-schottky analysis can be used to calculate the charge carrier density (N_D) from the slope based on the below Equation 1:[11]

$$N_D = (2/\varepsilon\varepsilon_0 e)(d_C^{-2}/d_v)^{-1} \quad (1)$$

C is the space charge capacitance, V is the potential, ε is the dielectric constant of hematite, ε_0 is the permittivity of vacuum, e is the electron charge. After introducing the Sn doping and a TiO_2 underlayer, N_D can be increased five times (2.9×10^{20} cm^{-3}) compared to the pristine FTO/α-Fe_2O_3 photoanode (5.5×10^{19} cm^{-3}). So it can prove that the Sn doping and a TiO_2 underlayer can increase carrier density.[12]

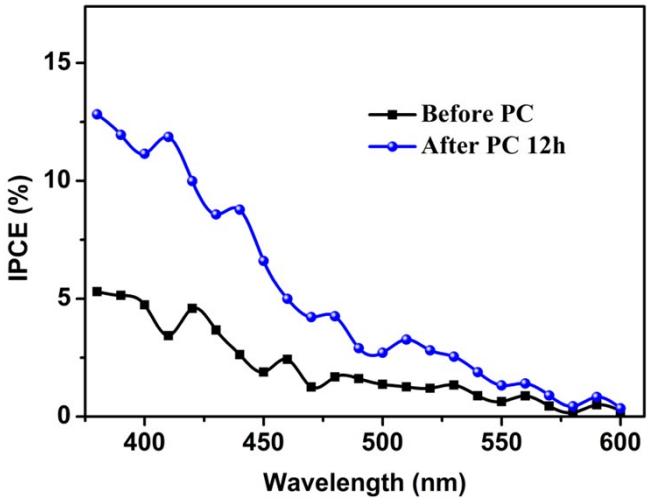

Fig. S7 IPCE spectra of FTO/TiO_2/Sn@α-Fe_2O_3 photoanode before and after PC for 12 h at 1.5V_{RHE}.

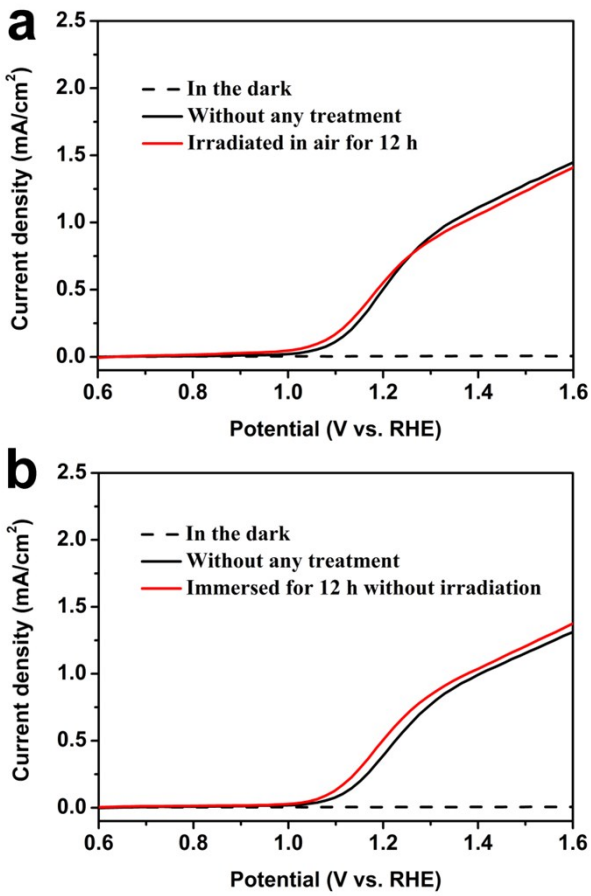

Fig. S8 (a) *J-E* curves of FTO/TiO_2/Sn@α-Fe_2O_3 photoanode irradiated by the AM 1.5G simulator in air for 12 h; (b) *J-E* curves of FTO/TiO_2/Sn@α-Fe_2O_3 photoanode immersed in 1 M NaOH solution without irradiation for 12 h.

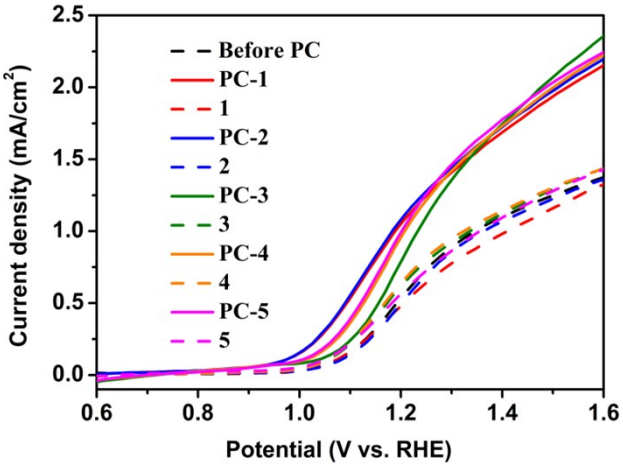

Fig. S9 Cyclic *J-E* test of FTO/TiO_2/Sn@α-Fe_2O_3 photoanode with being photocharged or discharged. One cycle is the photoanode was firstly discharged in the dark and in air for 12 h, and then photocharged in 1.0 M NaOH solution under AM 1.5G irradiation for 12 h.

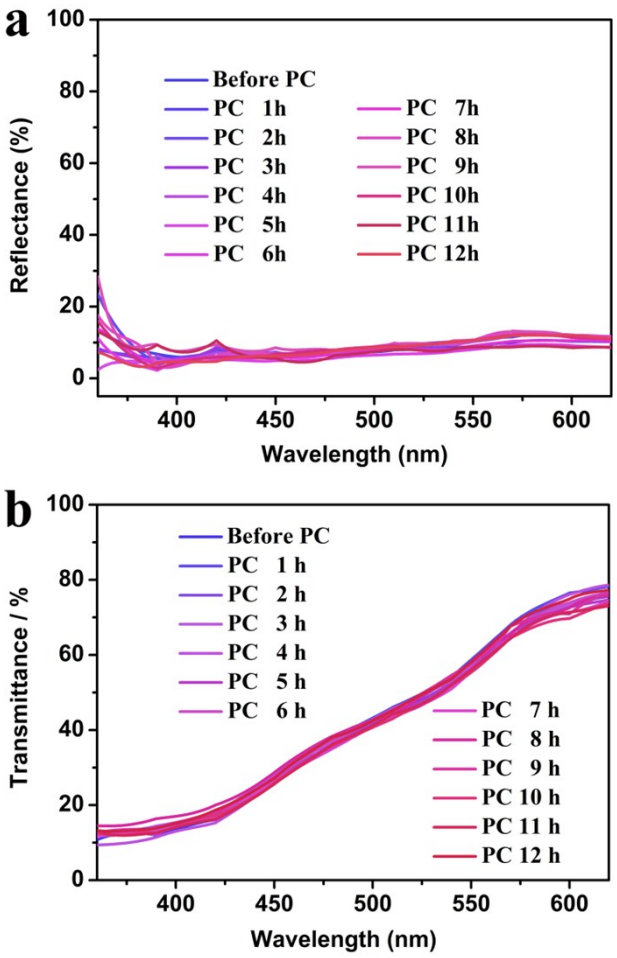

Fig. S10 Reflectance and transmissivity spectra of FTO/TiO_2/Sn@α-Fe_2O_3 photoanode in PC process for various durations.

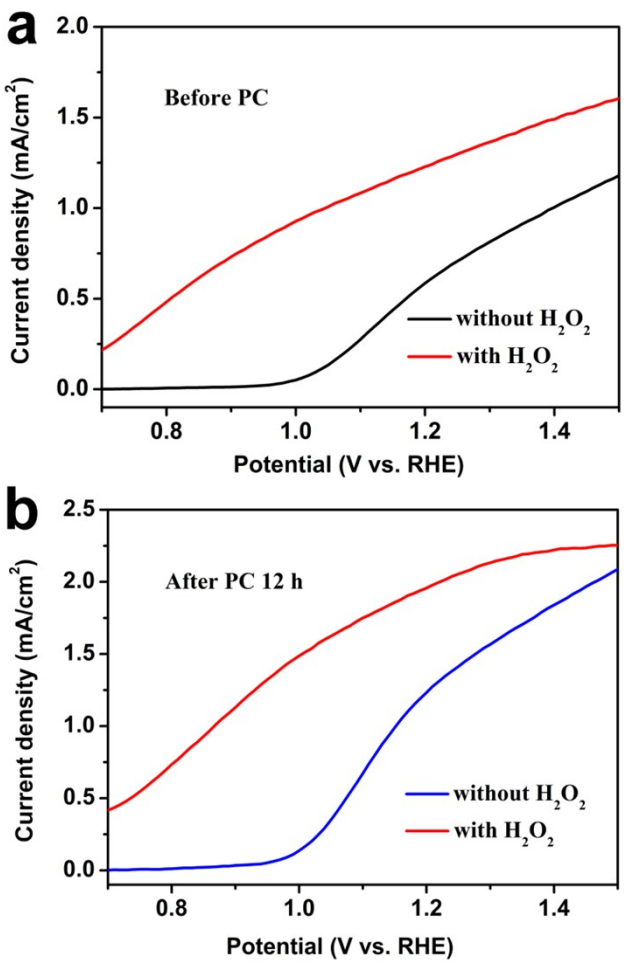

Fig. S11 *J-E* curves of FTO/TiO_2/Sn@α-Fe_2O_3 photoanode under AM 1.5G irradiation with and without H_2O_2 before (a) and after (b) PC for 12 h.

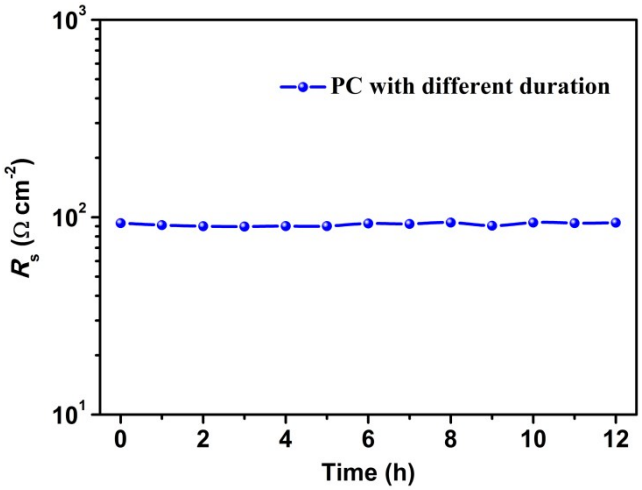

Fig. S12 R_s of FTO/TiO_2/Sn@α-Fe_2O_3 photoanode based on the equivalent circuit in PC process for various durations.

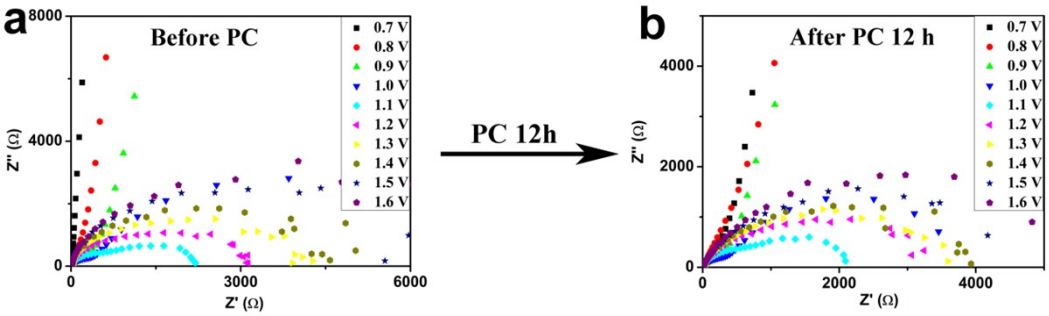

Fig. S13 Contrastive PEIS data of FTO/TiO_2/Sn@α-Fe_2O_3 photoanode before (a) and after PC for 12 h (b) measured at a bias from 0.7 V_{REH} to 1.6 V_{REH}.

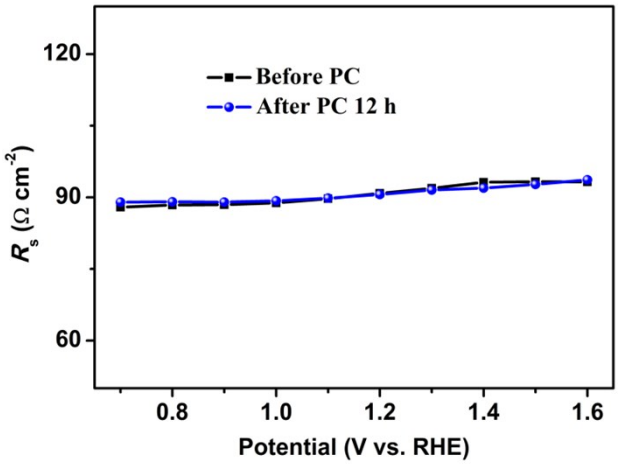

Fig. S14 R_s of FTO/TiO_2/Sn@α-Fe_2O_3 photoanode before and after PC for 12 h measured at a bias from 0.7 V_{REH} to 1.6 V_{REH}.

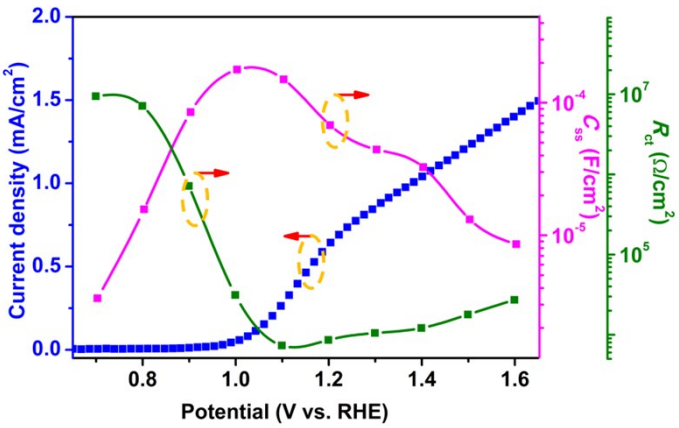

Fig. S15 Photocurrent onset potential of FTO/TiO_2/Sn@α-Fe_2O_3 photoanode before PC is consistent with the C_{ss} peak and the R_{ct} valley.

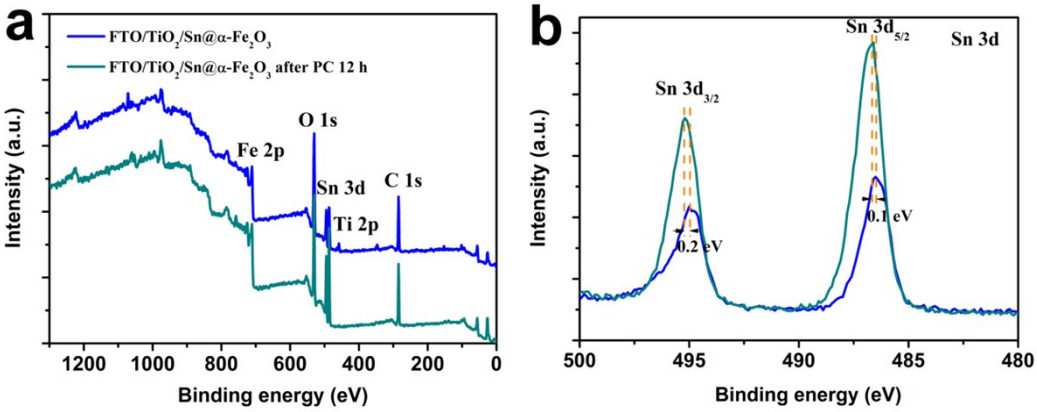

Fig. S16 XPS survey (a) and Sn 3d (b) core-level spectra of FTO/TiO_2/Sn@α-Fe_2O_3 photoanode before and after PC for 12 h.

References

1. J. Xie, P. Yang, X. Liang and J. Xiong, *ACS Appl. Energy Mater.*, 2018, **1**, 2769.
2. J. Deng, X. Lv and J. Zhong, *J. Phys. Chem. C*, 2018, **122**, 29268.
3. B. J. Trzesniewski and W. A. Smith, *J. Mater. Chem. A*, 2016, **4**, 2919.
4. B. J. Trzesniewski, I. A. Digdaya, T. Nagaki, S. Ravishankar, I. Herraiz-Cardona, D. A. Vermaas, A. Longo, S. Gimenez and W. A. Smith, *Energy Environ. Sci.*, 2017, **10**, 1517.
5. E. Y. Liu, J. E. Thorne, Y. He and D. Wang, *ACS Appl. Mater. Interfaces*, 2017, **9**, 22083.
6. T. Li, J. He, B. Pena and C. P. Berlinguette, *Angew. Chem. Int. Ed.*, 2016, **55**, 1769.
7. T. Li, J. He, B. Pena and C. P. Berlinguette, *ACS Appl. Mater. Interfaces*, 2016, **8**, 25010.
8. T. Zhang, Y. Liu, J. Liang and D. Wang, *Appl. Surf. Sci.*, 2017, **394**, 440.
9. S. C. Riha, B. M. Klahr, E. C. Tyo, S. Seifert, S. Vajda, M. J. Pellin, T. W. Hamann and A. B. F. Martinson, *ACS Nano*, 2013, **7**, 2396.
10. H. Zhang and C. Cheng, *ACS Energy Lett.*, 2017, **2**, 813.
11. A. K. Singh and D. Sarkar, *Nanoscale*, 2018, **10**, 13130.
12. X.-L. Zheng, C.-T. Dinh, F. P. G. D. Arquer, B. Zhang, M. Liu, O. Voznyy, Y.-Y. Li, G. Knight, S. Hoogland, Z.-H. Lu, X.-W. Du and E. H. Sargent, *Small*, 2016, **12**, 3181.